A Letters Journal Exploring the Frontiers of Physics

May 2014

EPL, **106** (2014) 37006 www.epljournal.org
doi: 10.1209/0295-5075/106/37006

Anderson localization of a Majorana fermion

D. A. Ivanov[1,2], P. M. Ostrovsky[3,4] and M. A. Skvortsov[4,5]

[1] *Institute for Theoretical Physics, ETH Zürich - 8093 Zürich, Switzerland*
[2] *Institute for Theoretical Physics, University of Zürich - 8057 Zürich, Switzerland*
[3] *Max Planck Institute for Solid State Research - Heisenbergstr. 1, 70569 Stuttgart, Germany*
[4] *L. D. Landau Institute for Theoretical Physics - 142432 Chernogolovka, Russia*
[5] *Moscow Institute of Physics and Technology - 141700 Moscow, Russia*

received 24 January 2014; accepted in final form 16 April 2014
published online 12 May 2014

PACS 74.45.+c – Proximity effects; Andreev reflection; SN and SNS junctions
PACS 73.20.Fz – Weak or Anderson localization
PACS 73.21.Hb – Electron states and collective excitations in multilayers, quantum wells, mesoscopic, and nanoscale systems: Quantum wires

Abstract – Isolated Majorana fermion states can be produced at the boundary of a topological superconductor in a quasi–one-dimensional geometry. If such a superconductor is connected to a disordered quantum wire, the Majorana fermion is spread into the wire, subject to Anderson localization. We study this effect in the limit of a thick wire with broken time-reversal and spin-rotational symmetries. With the use of a supersymmetric nonlinear sigma model, we calculate the average local density of states in the wire as a function of energy and of the distance from the interface with the superconductor. Our results may be qualitatively explained by the repulsion of states from the Majorana level and by Mott hybridization of localized states.

Introduction. – Recently, search for Majorana electron levels in solid-state systems has intensified, motivated by their potential use in quantum computing [1]. Several experimental groups reported indications of Majorana fermions in hybrid superconductor-semiconductor systems [2–5], which further stimulated theoretical studies of Majorana fermions in superconducting proximity structures.

One of the most promising proposals for detecting a Majorana level is based on the resonant Andreev reflection at zero energy [6,7]. The symmetry of the superconductor leads to the universal Andreev conductance $2e^2/h$ in the presence of a Majorana level. Due to the topological protection, the Majorana bound state and hence the resonance in the Andreev reflection are robust with respect to all sorts of local perturbations including disorder. Although the height of the resonance peak is universal (at low temperatures), its width is determined by the overlap of the Majorana wave function with electron states in the external probe. In order to be observed, the resonance peak should be reasonably narrow[1], which implies a localization of a Majorana level close to the Andreev interface. A possible experimental approach to localizing the Majorana level uses a tunnel barrier provided by suitably placed gates [2,3]. In the present paper, we suggest an alternative possibility: suppressing the escape of the Majorana mode by disorder-induced Anderson localization.

The effect of disorder in systems containing Majorana fermions was a subject of several recent papers addressing transport properties [8–11]. We complement those studies with an analysis of the average local density of states (LDOS): this quantity provides a direct information on the spatial profile of the Majorana mode and other electron states.

In a disordered wire, under an assumption of quantum coherence, the electronic states are localized [12], including the Majorana fermion. At the same time, the LDOS at low energies is modified, due to the level repulsion from the Majorana state (this effect was studied in detail in the zero-dimensional random-matrix limit [13,14]). In the case of a thick quasi–one-dimensional wire with a large number of channels, the modification of the density of states in the presence of a localized Majorana level can be accessed with the use of a supersymmetric nonlinear sigma model [15]. This approach was developed in ref. [16] to study the interplay of proximity and localization effects in conventional superconductor–normal-metal

[1] To be observable, the width of the resonance peak should be smaller than the superconducting gap and larger than the experimental energy resolution.

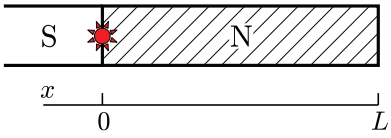

Fig. 1: (Color online) A disordered quantum wire (N) of length L coupled to a topological superconductor (S) at $x = 0$. The star marks the location of a Majorana fermion state. This state spreads at the localization length scale ξ into the wire and at the superconducting coherence length (which is assumed to be much shorter than ξ) into the superconductor.

junctions. An earlier study of the LDOS in Majorana quantum wires using the sigma-model formalism, without including localization effects, was performed in ref. [17].

In the present paper, we extend the calculation of ref. [16] to the case of a hybrid system consisting of a topological superconductor with a Majorana level and a wire with both time-reversal and spin symmetries broken, see fig. 1. We find the spatial structure of the localized Majorana state and the modification of the LDOS at low energies due to the level repulsion from the Majorana level. The localization of the Majorana level is similar to the localization of states in the bulk of the wire, and its level-repulsion effect extends to the Mott length scale. We further explain our results in terms of the Mott hybridization of localized states [18–21] and compare our findings to those in ref. [16].

Model. – We consider a junction between a topological superconductor and a normal disordered wire schematically shown in fig. 1. The wire has length L and the number of channels $N \gg 1$. Both the spin-rotational and time-reversal symmetry are assumed to be broken in the wire (at the length scales shorter than all other length scales of the theory). It therefore belongs to the symmetry class A (in Cartan notation [22]) and to the model IIb in Efetov's classifcation [23]. The superconductor is also assumed to have both time-reversal and spin-rotational symmetry broken and to be in a topological phase [24]. This superconducting symmetry class is usually denoted as B, D or BD [13,14,22,25]. We prefer to call this symmetry class B to emphasize the presence of a Majorana state at the boundary. An example of a microscopic Hamiltonian leading to such a symmetry can be found in refs. [26,27].

We assume quantum coherence in the wire, which leads to Anderson localization at the localization length $\xi = 2\pi\nu AD$ (here D is the diffusion coefficient in the wire, ν is the density of states, and A is the wire cross-section). Localization in the wire defines the energy scale $\Delta_\xi = D/\xi^2$ (of the order of the level spacing and of the Thouless energy at the length ξ). In short wires ($L \ll \xi$), another energy scale comes into play: the level spacing in the wire, $\delta = (2\nu AL)^{-1}$ (see footnote [2]). The localization of the Majorana fermion and the related level-repulsion effects occur at distances $x \lesssim \xi$ from the interface (up to logarithmic corrections, see the discussion of the Mott length (12) below) and at energies $E \lesssim \max(\Delta_\xi, \delta)$ around the Fermi level, as in the non-topological case [16]. We further assume these conditions on x and E.

The interface between such a superconductor and a wire may be described in terms of a scattering matrix $2N\times 2N$, which involves both normal and Andreev reflections. We assume a large total Andreev conductance. We also assume that the gap in the superconducting part of the junction is much larger than the energy scales Δ_ξ and δ. Then, within the window of energies considered, we may neglect the energy dependence of the Andreev scattering matrix (the limit of a broad "Majorana resonance" [6,7]). The symmetry properties of such a scattering matrix are discussed in detail in refs. [8,11,24]. Similarly to the results of ref. [16], we find that the role of the Andreev interface, in this high-transparency limit, is to fully suppress the soft localization modes (diffusons and cooperons) incompatible with the symmetry of the superconductor. At such an interface, the boundary conditions for the supersymmetric nonlinear sigma model describing the wire take a particularly simple form (see the following section).

Density of states: general formalism. – Our main object of study is the disorder-averaged local density of states $\langle\rho_E(x)\rangle$ (normalized to the bulk value in the wire). Following ref. [16], we express it as an expectation value in a supersymmetric nonlinear sigma model [23],

$$\langle\rho_E(x)\rangle = \frac{1}{4}\,\mathrm{Re}\int \mathrm{str}\,(k\Lambda Q(x))\,e^{-S[Q]}DQ. \qquad (1)$$

Here Q is the supersymmetric 4×4 matrix acting in the product of the Fermi-Bose (FB) and retarded-advanced (RA) two-dimensional spaces and subject to the constraint $Q^2 = 1$ (this space of Q matrices corresponds to the symmetry class A [22]). The matrix $\Lambda = \sigma_z^{\mathrm{RA}}$ is the metallic saddle point of the sigma model, and the supersymmetry-breaking matrix $k = \sigma_z^{\mathrm{FB}}$ (we follow the notations of ref. [23]). The supersymmetric action has the form

$$S[Q] = \frac{\pi\nu A}{4}\int_0^L \mathrm{d}x\ \mathrm{str}\left[D(\nabla Q)^2 + 4iE\Lambda Q\right]. \qquad (2)$$

At the interface with the superconductor (at $x = 0$), under the assumptions specified in the previous section, the matrix Q is restricted to the symmetry class of the combination of the symmetries in the wire and in the superconductor (class B in our case).

The one-dimensional sigma model (1) can be solved analytically by mapping onto an imaginary-time quantum mechanics on the target space of Q matrices [28]. The relevant degrees of freedom of the Q matrix are the eigenvalues of its RR block, λ_F and λ_B [23]. The fermionic parameter λ_F takes values between -1 and 1 (compact), and the bosonic component λ_B between 1 and $+\infty$ (non-compact). At the interface with a superconductor, the

[2]The 1/2 factor in the definition of the level spacing δ takes into account the doubling of levels due to Andreev reflections and is included for consistency of notations with refs. [14,16,25].

Q matrix is reduced to that of the symmetry class B or D (depending on the presence or absence of a Majorana level), which constrains the FF block to two points only: $\lambda_F = \pm 1$ [13,14,16]. As derived in ref. [16], in the case of class D (no Majorana level), the two components of the functional integral (1) corresponding to $\lambda_F(x{=}0) = 1$ and $\lambda_F(x{=}0) = -1$ must be added with opposite signs. In ref. [14], it was remarked that the difference between the presence and absence of the Majorana mode corresponds to reversing the relative sign between the functional integrals over the two disconnected components of the space of Q matrices. Therefore, we conclude that, in the case of class B (with the Majorana mode), the average LDOS is given by reversing the relative sign in eq. (29) of ref. [16]:

$$\langle \rho_E(x) \rangle = 1 + \mathrm{Re} \int_1^\infty \mathrm{d}\lambda_B \, \frac{\Psi(1, \lambda_B; x) + \Psi(-1, \lambda_B; x)}{2}. \tag{3}$$

The wave function $\Psi(\lambda_F, \lambda_B; x)$ results from evaluation of the functional integral (1) by the transfer-matrix technique of Efetov and Larkin [28] and is defined as [29,30]

$$\Psi(\lambda_F, \lambda_B; x) = e^{-2\tilde{H}x/\xi} e^{-2H(L-x)/\xi} \cdot 1. \tag{4}$$

The Hamiltonians $\tilde{H}$ and H governing the evolution of the wave function are given by

$$\tilde{H} = \tilde{H}_B + \tilde{H}_F, \quad H = (\lambda_B - \lambda_F)\tilde{H}(\lambda_B - \lambda_F)^{-1}, \tag{5}$$

where

$$\tilde{H}_B = -\frac{1}{2}\frac{\partial}{\partial \lambda_B}(\lambda_B^2 - 1)\frac{\partial}{\partial \lambda_B} + \frac{\kappa^2}{16}\lambda_B, \tag{6a}$$

$$\tilde{H}_F = -\frac{1}{2}\frac{\partial}{\partial \lambda_F}(1 - \lambda_F^2)\frac{\partial}{\partial \lambda_F} - \frac{\kappa^2}{16}\lambda_F, \tag{6b}$$

and we define $\kappa^2 = -8iE/\Delta_\xi$.

Short-wire limit. – In the limit of a short wire, $L \ll \min(\xi, \sqrt{D/E})$, the gradient terms in the Hamiltonian (5) may be neglected [16], and a simple calculation leads to the well-known result for the random-matrix ensemble of class B [14,17,31]:

$$\langle \rho_E(x) \rangle = 1 - \frac{\sin(2\pi E/\delta)}{(2\pi E/\delta)} + \delta\,(E/\delta)\,. \tag{7}$$

The Majorana level reveals itself as a delta-function term in the density of states. The integral weight of this delta peak equals 1/2, which reflects the Majorana nature of this electronic level.

Semi-infinite–wire limit. – In the limit of a semi-infinite wire, at low energies ($E \ll \Delta_\xi$), the calculation can be performed using the technique developed in ref. [30]. Taking the limit $L \to \infty$ in eq. (4) results in

$$\Psi(\lambda_F, \lambda_B; x)_{L\to\infty} = e^{-2(\tilde{H}_F + \tilde{H}_B)x/\xi}\, \Psi_0(\lambda_F, \lambda_B), \tag{8}$$

where

$$\Psi_0(\lambda_F, \lambda_B) = I_0(q)\, pK_1(p) + qI_1(q)\, K_0(p) \tag{9}$$

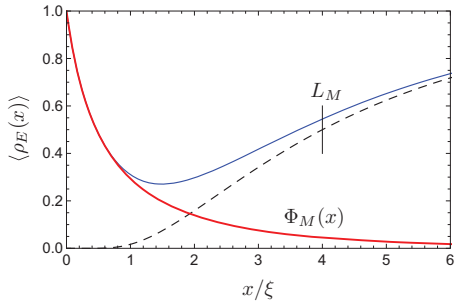

Fig. 2: (Color online) Sketch of the average LDOS $\langle \rho_E(x) \rangle$ in the semi-infinite–wire limit ($L \to \infty$) at a small finite energy E as a function of x (thin blue curve), as given by eq. (10). Close to the interface, it follows the profile of the Majorana mode $\Phi_M(x)$ (thick red curve). At $x \sim L_M$, the LDOS exhibits a crossover given by the erf function (dashed black line).

(with $p = \kappa\sqrt{(\lambda_B + 1)/2}$ and $q = \kappa\sqrt{(\lambda_F + 1)/2}$) is the zero mode of the Hamiltonian H found in ref. [32].

Since the bosonic and fermionic degrees of freedom separate, the calculation may be further performed perturbatively in the fermionic sector (in the limit of $E \ll \Delta_\xi$) and by expanding in the basis of eigenstates of $\tilde{H}_B$ in the bosonic sector [30]. The details of the calculation can be found in the Appendix. The result has the form

$$\langle \rho_E(x) \rangle = \Phi_M(x) + \frac{1}{2}\left[1 + \mathrm{erf}\left(\frac{x - L_M}{2\sqrt{x\,\xi}}\right)\right] + \Phi_M(x)\, \pi\, \delta(E/\Delta_\xi). \tag{10}$$

The last δ term in eq. (10) corresponds to the localized Majorana mode whose profile is given by

$$\Phi_M(x) = 2\pi \int_0^\infty k\,\mathrm{d}k\, \frac{\sinh \pi k}{\cosh^2 \pi k}(k^2 + 1/4) e^{-(x/\xi)(k^2+1/4)}, \tag{11}$$

and

$$L_M = 2\xi \ln(\Delta_\xi/E) \tag{12}$$

is the Mott length scale [18]. Note that the profile of the Majorana level $\Phi_M(x)$ contributes not only to the delta peak at zero energy, but also to the background LDOS at small finite energies (see our discussion of Mott hybridization below). The function $\langle \rho_E(x) \rangle$ is plotted in fig. 2.

As in the short-wire limit, one can verify that the integral weight of the Majorana delta peak in the LDOS (10) equals 1/2. The *average* intensity of the Majorana mode decays away from the interface at the length scale 4ξ, similar to the statistics of a single localized wave function [28,30,33]. On general grounds, we believe that the statistics of the tails of this localized state is log-normal [21] with the *typical* Majorana state decaying at the length scale ξ. Note however that the exact form of the average intensity of the Majorana state (11) differs from the two-point correlation function of the intensity of a single localized state (eq. (75) of ref. [30], see also refs. [28,33]).

We can also remark a similarity of the LDOS profile (10) to the two-point LDOS correlation function in

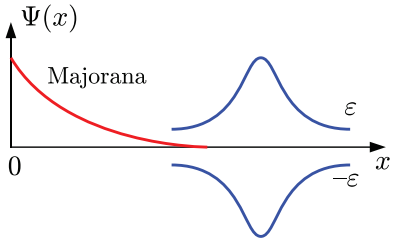

Fig. 3: (Color online) A schematic representation of the three localized states whose hybridization is responsible for $\langle\rho_E(x)\rangle$ at small, but finite energies E.

the quasi–one-dimensional wire [20,21,30]. Namely, at low energies, it consists of two parts: the "short-range" part localized at the length scale ξ and proportional to the single-particle statistics [$\Phi_M(x)$ in our case] and the "long-range" part at the length scale L_M. As in the case of a quasi–one-dimensional wire, this structure may be easily understood in terms of a Mott hybridization of localized states [18–21]. The difference from the two-point correlation case considered in ref. [21] is that now three states hybridize: the Majorana state and the pair of particle-hole (Bogoliubov–de-Gennes) symmetric [22,25] states at energies ε and $-\varepsilon$ (see fig. 3). The hybridization Hamiltonian involving these three states has the form

$$H_{\rm hybrid} = \begin{pmatrix} \varepsilon & J & 0 \\ J^* & 0 & J^* \\ 0 & J & -\varepsilon \end{pmatrix}, \qquad (13)$$

where the *typical* value of the hybridization matrix element J is $\Delta_\xi e^{-x/(2\xi)}$ (note that there is no direct hybridization between the state at energy ε and its image in the symmetry class B [25]). Following the argument of ref. [21], we conclude that this hybridization mechanism produces a crossover between $\rho_E(x) = 0$ and $\rho_E(x) = 1$ at $x = L_M$, in agreement with the result (10) of our calculation. Following the same argument, the hybridized states reproduce the Majorana wave function at $x \lesssim \xi$, and therefore $\langle\rho_E(x)\rangle$ must be proportional to the average intensity of the Majorana state $\Phi_M(x)$ in this region of x, again in agreement with eq. (10).

It is instructive to compare this situation with that in superconductor–normal-metal (SN) junctions in the symmetry classes C and D considered in ref. [16]. In class D, there is no hybridization between any state and its particle-hole mirror image [25]. Since there is no state at $E = 0$, this implies no repulsion from the Fermi level, and $\langle\rho_E(x)\rangle$ is enhanced at low energies at $x \lesssim \xi$ (with $\langle\rho_{E\to 0}(0)\rangle = 3$). In class C, the particle-hole mirror images hybridize and repel each other, and therefore $\langle\rho_E(x)\rangle$ is suppressed at $x < L_M/2$ (as opposed to $x < L_M$ in class B), since hybridization involves an electron (hole) propagating to the SN interface and back. The comparison of the three classes is presented in table 1.

We remark that finite limits $\langle\rho_{E\to 0}(x)\rangle$ in classes B and D reported in table 1 are only achieved if the limit $L \to \infty$ is taken before $E \to 0$. If one considers the opposite order of limits, (*i.e.*, $E \to 0$ at a finite L), then the repulsion from the Fermi level leads to $\langle\rho_{E\to 0}(x)\rangle = 0$. In fact, in a finite wire, the hybridization is only possible at distances $x < L$, which sets the energy scale $E_g \sim \Delta_\xi e^{-L/(2\xi)}$ in class B (and $E_g \sim \Delta_\xi e^{-L/\xi}$ in class C) as the typical minimum energy of hybridized states. Below this energy scale, the density of states is suppressed, which is reminiscent of a minigap in conventional SN junctions [34]. In a finite wire, at very small energies ($E \ll E_g$), the LDOS scales as $\langle\rho_{E\to 0}(x)\rangle \propto |E|^\alpha$. A finite value of α indicates repulsion either from the Majorana state or from the Bogoliubov–de-Gennes mirror image: it equals the number of independent degrees of freedom in the possible hybridization matrix element between the two repelling states. The values of α are included in table 1 for completeness. They are also known from the random matrix theory for all symmetry classes (refs. [14,25,31] and references therein).

Table 1: Level repulsion and Mott hybridization in normal-metal–superconductor junctions of the symmetry classes B, D, and C in the limit of a semi-infinite wire $L \to \infty$.

Class	Majorana	α	Hybrid. length	$\langle\rho_{E\to 0}(0)\rangle$
B	Yes	2	$2\xi \ln(\Delta_\xi/E)$	1
D	No	0	—	3
C	No	2	$\xi \ln(\Delta_\xi/E)$	0

Discussion. – To summarize, we have analytically solved the problem of Anderson localization of a Majorana fermion in a wire with time-reversal and spin-rotational symmetries broken. We find that the Majorana level gets localized in a way qualitatively similar to other electronic states and contributes to the repulsion of other electron levels from the Fermi energy near the SN interface. We expect that, at a qualitative level, these properties are universal: they do not depend on the details of geometry and on the symmetry class of the wire. Moreover, since the statistics of the envelope of a single localized wave function in quasi–one-dimensional geometry is independent of the symmetry class [35] and since the behavior at the Mott length scale is determined by the hybridization physics [18–21], we believe that our results (10) and (11) are universally valid also for wires with orthogonal and symplectic (with an even number of channels [36]) symmetries, as long as a Majorana level is present at the SN interface.

Our results may be useful for possible qubit designs involving Majorana fermions localized by disorder. The intensity $\Phi_M(x)$ of the Majorana state may be probed by tunneling experiments (while the maximum of the tunneling peak at zero temperature must equal $2e^2/h$, according to ref. [6], its width and temperature smearing are sensitive to the amplitude $\Phi_M(x)$ [7]). Also, the profile of $\Phi_M(x)$ would be relevant for hybridization of Majorana fermions, if two of them are placed at the opposite ends of

the wire (similarly to the case of a superconducting wire considered in ref. [37]).

* * *

This work was partially supported by the program "Quantum mesoscopic and disordered structures" of the RAS, RFBR grant No. 13-02-01389, the German Ministry of Education and Research (BMBF), and the Swiss National Foundation through the NCCR QSIT.

Appendix: details of the calculation. – Here we provide the details of the calculation leading to the results (10) and (11) for the LDOS in the infinite-wire limit. The calculation extensively uses the techniques developed in ref. [30]. In the fermionic sector, the calculation is done perturbatively, while in the bosonic sector we use the Poisson summation formula involving the scattering matrix for the Hamiltonian $\tilde{H}_B$ (eq. (6a)). It will be convenient to perform the calculation in the variables p and q introduced below eq. (9). We also introduce the dimensionless coordinate $t = x/\xi$. The main idea of the calculation is to keep track of the relevant orders in κ.

The starting point of the calculation are eqs. (3), (8), and (9). The Hamiltonians (6a) and (6b) in the variables p and q read

$$\tilde{H}_B = \frac{1}{8}\left[\frac{1}{p}\frac{\partial}{\partial p}p(\kappa^2-p^2)\frac{\partial}{\partial p}+p^2-\frac{\kappa^2}{2}\right], \quad \text{(A.1)}$$

$$\tilde{H}_F = \frac{1}{8}\left[\frac{1}{q}\frac{\partial}{\partial q}q(q^2-\kappa^2)\frac{\partial}{\partial q}-q^2+\frac{\kappa^2}{2}\right]. \quad \text{(A.2)}$$

In the fermionic sector, we expand the wave function in powers of κ and q:

$$\Psi(q,p;t) = \psi_0(p,t) + q^2\psi_1(p,t) + \kappa^2\psi_2(p,t) + \ldots, \quad \text{(A.3)}$$

which, upon substitution into eq. (3), results in

$$\langle\rho_E(x)\rangle = 1 + \frac{1}{2}\,\mathrm{Re}\int \mathrm{d}\lambda_B\,\big[2\psi_0(p,t) + \kappa^2\psi_1(p,t) + 2\kappa^2\psi_2(p,t) + \ldots\big]. \quad \text{(A.4)}$$

The Hamiltonian $\tilde{H}_F$ acts as

$$\tilde{H}_F\big[\psi_0 + q^2\psi_1 + \kappa^2\psi_2\big] = (q^2-\kappa^2/2)\big[-\psi_0/8 + \psi_1\big] + o(q^2,\kappa^2), \quad \text{(A.5)}$$

which allows us to represent it by a finite matrix in the basis $(1, q^2, \kappa^2)$:

$$\tilde{H}_F\begin{pmatrix}\psi_0\\ \psi_1\\ \psi_2\end{pmatrix} = \begin{pmatrix}0 & 0 & 0\\ -1/8 & 1 & 0\\ 1/16 & -1/2 & 0\end{pmatrix}\begin{pmatrix}\psi_0\\ \psi_1\\ \psi_2\end{pmatrix} + o(q^2,\kappa^2). \quad \text{(A.6)}$$

Exponentiating this matrix, we obtain

$$e^{-2\tilde{H}_F t}\Big[\psi_0 + q^2\psi_1 + \kappa^2\psi_2\Big] = \psi_0 + q^2\left[\frac{1-e^{-2t}}{8}\psi_0 + e^{-2t}\psi_1\right] + \kappa^2\left[\frac{e^{-2t}-1}{16}\psi_0 + \frac{1-e^{-2t}}{2}\psi_1 + \psi_2\right] + o(q^2,\kappa^2). \quad \text{(A.7)}$$

Applying this operation to the zero-mode wave function

$$\Psi_0(q,p) = pK_1(p) + q^2\left(\frac{K_0(p)}{2} + \frac{pK_1(p)}{4}\right) + o(q^2) \quad \text{(A.8)}$$

yields

$$e^{-2\tilde{H}_F t}\Psi_0(q,p) = pK_1(p) + q^2\left[\frac{1+e^{-2t}}{8}pK_1(p) + \frac{e^{-2t}}{2}K_0(p)\right] + \kappa^2\left[\frac{1-e^{-2t}}{16}pK_1(p) + \frac{1-e^{-2t}}{4}K_0(p)\right] + o(q^2,\kappa^2). \quad \text{(A.9)}$$

Inserting this result into eq. (A.4), we obtain

$$\langle\rho_E(x)\rangle = 1 + \mathrm{Re}\int \mathrm{d}\lambda_B\, e^{-2\tilde{H}_B t}\Big(pK_1(p) + (\kappa^2/8)\big[pK_1(p) + 2K_0(p)\big]\Big). \quad \text{(A.10)}$$

This equation is valid up to corrections of order $o(\kappa^2)$ in the integrand, which results in corrections of order $o(1)$ for $\langle\rho_E(x)\rangle$ (the integration over λ_B extends to $\lambda_B \sim \kappa^{-2}$ and thus brings in a large κ^{-2} factor). It remains now to calculate the evolution with respect to the bosonic part of the Hamiltonian $\tilde{H}_B$.

We further calculate the following two matrix elements:

$$\begin{Bmatrix} M_1 \\ M_0 \end{Bmatrix} = \int \mathrm{d}\lambda_B\, e^{-2\tilde{H}_B t}\begin{Bmatrix} pK_1(p) \\ K_0(p) \end{Bmatrix} \quad \text{(A.11)}$$

using the method developed in ref. [30]. From eq. (A.10) we see that the integral involving $pK_1(p)$ should be calculated up to two leading terms in small energy expansion, $O(1/\kappa^2)$ and $O(1)$, while for the second integral it suffices to extract only the main $O(1/\kappa^2)$ asymptotics.

We use the general expansion of the evolution operator in the eigenfunctions of $\tilde{H}_B$

$$\begin{Bmatrix} M_1 \\ M_0 \end{Bmatrix} = \sum_k \frac{\langle 1|\phi_k\rangle}{\langle\phi_k|\phi_k\rangle} e^{-2E_k t}\begin{Bmatrix} \langle\phi_k|pK_1(p)\rangle \\ \langle\phi_k|K_0(p)\rangle \end{Bmatrix} \quad \text{(A.12)}$$

and pick all the necessary ingredients from ref. [30]:

$$\langle\phi_k|pK_1(p)\rangle = \frac{\pi}{\kappa\cosh\pi k}\left[1 + 4k^2 - \frac{\kappa^2}{2} + O(\kappa^4)\right], \quad \text{(A.13)}$$

$$\langle\phi_k|K_0(p)\rangle = \frac{2\pi}{\kappa\cosh\pi k}\left[1 + O(\kappa^4)\right], \quad \text{(A.14)}$$

$$\langle\phi_k|\phi_k\rangle = -\frac{i}{2\pi}\coth\pi k\frac{\partial\ln S(k)}{\partial k}\left[\frac{1}{k} + O(\kappa^4)\right], \quad \text{(A.15)}$$

$$\sum_k \cdots = -\frac{i}{2\pi}\sum_{n=-\infty}^{+\infty}\int_0^\infty \mathrm{d}k\, S^n(k)\frac{\partial\ln S(k)}{\partial k}\cdots, \quad \text{(A.16)}$$

$$S(k) = \left(\frac{\kappa^2}{4}\right)^{-2ik}\left[\frac{\Gamma(2ik)\Gamma(1/2-ik)}{\Gamma(-2ik)\Gamma(1/2+ik)}\right]^2\left[1 + O(\kappa^4)\right], \quad \text{(A.17)}$$

$$E_k = 1/8 + k^2/2 + O(\kappa^4). \quad \text{(A.18)}$$

The only missing piece is $\langle 1|\phi_k\rangle$. It can be easily computed along the lines of Appendix C of ref. [30]:

$$\langle 1|\phi_k\rangle = \int \mathrm{d}\lambda_B\, \phi_k = (4/\kappa)\left[1 + O(\kappa^4)\right]. \qquad \text{(A.19)}$$

Putting everything together, we obtain

$$M_1 = 4\pi \int_0^\infty k\,\mathrm{d}k\, \frac{\sinh \pi k}{\cosh^2 \pi k} \sum_{n=-\infty}^{+\infty} S^n(k) \times \left[(1+4k^2)/\kappa^2 - 1/2 + O(\kappa^2)\right] e^{-t(k^2+1/4)}. \qquad \text{(A.20)}$$

The term with $n = 0$ rapidly converges as an integral over real k, while $n = \pm 1$ terms oscillate and are determined by the competition between the pole at $k = i/2$ and of the saddle point $k_* = it_M/2t$ with $t_M = 4\ln(2/\kappa)$. The pole contribution is dominant at $t \ll t_M$ and yields -1. The saddle point k_* becomes important at $t \sim t_M$ and provides a step-like "erf term". The result is

$$M_1 = -\frac{1}{2} + \frac{1}{2}\,\mathrm{erf}\left(\frac{t - t_M}{2\sqrt{t}}\right) + 4\pi \int_0^\infty k\,\mathrm{d}k\, \frac{\sinh \pi k}{\cosh^2 \pi k} \left[\frac{1+4k^2}{\kappa^2} - \frac{1}{2}\right] e^{-t(k^2+1/4)} + O(\kappa^2). \qquad \text{(A.21)}$$

Evolution of $K_0(p)$ is easier since we need only the leading term. Setting $n = 0$, we find

$$M_0 = \frac{8\pi}{\kappa^2} \int_0^\infty k\,\mathrm{d}k\, \frac{\sinh \pi k}{\cosh^2 \pi k} e^{-t(k^2+1/4)} + O(1). \qquad \text{(A.22)}$$

The results (10) and (11) for the LDOS are now obtained in a straightforward way by substituting the integrals (A.21) and (A.22) into eq. (A.10). The Majorana delta peak arises from $\mathrm{Re}(1/\kappa^2) = (\pi/8)\delta(E/\Delta_\xi)$.

REFERENCES

[1] Beenakker C. W., *Annu. Rev. Condens. Matter Phys.*, **4** (2013) 113.
[2] Mourik V., Zuo K., Frolov S. M., Plissard S. R., Bakkers E. P. A. M. and Kouwenhoven L. P., *Science*, **336** (2012) 1003.
[3] Das A., Ronen Y., Most Y., Oreg Y., Heiblum M. and Shtrikman H., *Nat. Phys.*, **8** (2012) 887.
[4] Deng M. T., Yu C. L., Huang G. Y., Larsson M., Caroff P. and Xu H. Q., *Nano Lett.*, **12** (2012) 6414.
[5] Rokhinson L. P., Liu X. and Furydna J. K., *Nat. Phys.*, **8** (2012) 795.
[6] Law K. T., Lee P. A. and Ng T. K., *Phys. Rev. Lett.*, **103** (2009) 237001.
[7] Ioselevich P. A. and Feigel'man M. V., *New J. Phys.*, **15** (2013) 055011.
[8] Akhmerov A. R., Dahlhaus J. P., Hassler F., Wimmer M. and Beenakker C. W. J., *Phys. Rev. Lett.*, **106** (2011) 057001.
[9] Wimmer M., Akhmerov A. R., Dahlhaus J. P. and Beenakker C. W. J., *New J. Phys.*, **13** (2011) 053016.
[10] Liu J., Potter A. C., Law K. T. and Lee P. A., *Phys. Rev. Lett.*, **109** (2012) 267002.
[11] Pikulin D. I., Dahlhaus J. P., Wimmer M., Schomerus H. and Beenakker C. W., *New J. Phys.*, **14** (2012) 125011.
[12] Anderson P. W., *Phys. Rev.*, **109** (1958) 1492.
[13] Bocquet M., Serban D. and Zirnbauer M. R., *Nucl. Phys. B*, **578** (2000) 628.
[14] Ivanov D. A., *J. Math. Phys.*, **43** (2002) 126.
[15] Efetov K. B., *Adv. Phys.*, **32** (1983) 53.
[16] Skvortsov M. A., Ostrovsky P. M., Ivanov D. A. and Fominov Ya. V., *Phys. Rev. B*, **87** (2013) 104502.
[17] Bagrets D. and Altland A., *Phys. Rev. Lett.*, **109** (2012) 227005.
[18] Mott N. F., *Philos. Mag.*, **17** (1968) 1259; **22** (1970) 7.
[19] Sivan U. and Imry Y., *Phys. Rev. B*, **35** (1987) 6074.
[20] Altland A. and Fuchs D., *Phys. Rev. Lett.*, **74** (1995) 4269.
[21] Ivanov D. A., Skvortsov M. A., Ostrovsky P. M. and Fominov Ya. V., *Phys. Rev. B*, **85** (2012) 035109.
[22] Zirnbauer M. R., *J. Math. Phys.*, **37** (1996) 4986.
[23] Efetov K. B., *Supersymmetry in Disorder and Chaos* (Cambridge University Press, New York) 1997.
[24] Beenakker C. W. J., Dahlhaus J. P., Wimmer M. and Akhmerov A. R., *Phys. Rev. B*, **83** (2011) 085413.
[25] Altland A. and Zirnbauer M. R., *Phys. Rev. B*, **55** (1997) 1142.
[26] Lutchyn R. M., Sau J. D. and Das Sarma S., *Phys. Rev. Lett.*, **105** (2010) 077001.
[27] Oreg Y., Refael G. and von Oppen F., *Phys. Rev. Lett.*, **105** (2010) 177002.
[28] Efetov K. B. and Larkin A. I., *Zh. Eksp. Teor. Fiz.*, **85** (1983) 764 (*Sov. Phys. JETP*, **58** (1983) 444).
[29] Ivanov D. A. and Skvortsov M. A., *J. Phys. A: Math. Theor.*, **41** (2008) 215003.
[30] Ivanov D. A., Ostrovsky P. M. and Skvortsov M. A., *Phys. Rev. B*, **79** (2009) 205108.
[31] Mehta M. L., *Random Matrices* (Academic Press, Boston) 1991.
[32] Skvortsov M. A. and Ostrovsky P. M., *Pis'ma Zh. Eksp. Teor. Fiz.*, **85** (2007) 79 (*JETP Lett.*, **85** (2007) 72).
[33] Gogolin A. A., *Zh. Eksp. Teor. Fiz.*, **71** (1976) 1912 (*Sov. Phys. JETP*, **44** (1976) 1003).
[34] Golubov A. A. and Kupriyanov M. Yu., *Zh. Eksp. Teor. Fiz.*, **96** (1989) 1420 (*Sov. Phys. JETP*, **69** (1989) 805).
[35] Mirlin A. D., *J. Math. Phys.*, **38** (1997) 1888; Mirlin A. D., *Phys. Rep.*, **326** (2000) 259.
[36] Brouwer P. W. and Frahm K., *Phys. Rev. B*, **53** (1996) 1490; Takane Y., *J. Phys. Soc. Jpn.*, **73** (2004) 1430.
[37] Brouwer P. W., Duckheim M., Romito A. and von Oppen F., *Phys. Rev. Lett.*, **107** (2011) 196804.